

Extracellular serine and glycine are required for mouse and human skeletal muscle stem and progenitor cell function



Brandon J. Gheller¹, Jamie E. Blum¹, Esther W. Lim², Michal K. Handzlik², Ern Hwei Hannah Fong³, Anthony C. Ko¹, Shray Khanna¹, Molly E. Gheller¹, Erica L. Bender¹, Matthew S. Alexander^{4,5,6,7}, Patrick J. Stover⁸, Martha S. Field¹, Benjamin D. Cosgrove³, Christian M. Metallo², Anna E. Thalacker-Mercer^{1,5,9,*}

ABSTRACT

Objective: Skeletal muscle regeneration relies on muscle-specific adult stem cells (MuSCs), MuSC progeny, muscle progenitor cells (MPCs), and a coordinated myogenic program that is influenced by the extracellular environment. Following injury, MPCs undergo a transient and rapid period of population expansion, which is necessary to repair damaged myofibers and restore muscle homeostasis. Certain pathologies (e.g., metabolic diseases and muscle dystrophies) and advanced age are associated with dysregulated muscle regeneration. The availability of serine and glycine, two nutritionally non-essential amino acids, is altered in humans with these pathologies, and these amino acids have been shown to influence the proliferative state of non-muscle cells. Our objective was to determine the role of serine/glycine in MuSC/MPC function.

Methods: Primary human MPCs (*hMPCs*) were used for *in vitro* experiments, and young (4–6 mo) and old (>20 mo) mice were used for *in vivo* experiments. Serine/glycine availability was manipulated using specially formulated media *in vitro* or dietary restriction *in vivo* followed by downstream metabolic and cell proliferation analyses.

Results: We identified that serine/glycine are essential for *hMPC* proliferation. Dietary restriction of serine/glycine in a mouse model of skeletal muscle regeneration lowered the abundance of MuSCs 3 days post-injury. Stable isotope-tracing studies showed that *hMPCs* rely on extracellular serine/glycine for population expansion because they exhibit a limited capacity for *de novo* serine/glycine biosynthesis. Restriction of serine/glycine to *hMPCs* resulted in cell cycle arrest in G0/G1. Extracellular serine/glycine was necessary to support glutathione and global protein synthesis in *hMPCs*. Using an aged mouse model, we found that reduced serine/glycine availability augmented intermyocellular adipocytes 28 days post-injury.

Conclusions: These studies demonstrated that despite an absolute serine/glycine requirement for MuSC/MPC proliferation, *de novo* synthesis was inadequate to support these demands, making extracellular serine and glycine conditionally essential for efficient skeletal muscle regeneration.

© 2020 The Authors. Published by Elsevier GmbH. This is an open access article under the CC BY-NC-ND license (<http://creativecommons.org/licenses/by-nc-nd/4.0/>).

Keywords Muscle; Muscle regeneration; Muscle stem cell; Muscle progenitor cell; Proliferation; Muscle metabolism; Serine metabolism; Glycine metabolism; Protein synthesis

1. INTRODUCTION

Skeletal muscle regeneration relies on muscle-specific adult stem and progenitor cells (MuSCs and MPCs, respectively) [1] and an orchestrated myogenic program that includes intracellular and extracellular cues. MuSCs reside in a quiescent state, are activated after injury, and produce a transient and rapidly expanding population of committed MPCs. Under healthy conditions, MPC population expansion provides an adequate number of cells to donate nuclei to damaged myofibers or

create nascent myofibers, thereby restoring homeostasis. However, with advancing age [2] and chronic conditions including chronic kidney disease (CKD) [3], type I diabetes [4,5], and muscle dystrophy [6], skeletal muscle regeneration is diminished. The failure of skeletal muscle regeneration is largely driven by impairment of MuSC/MPC function [7] due to both cell-extrinsic and cell-intrinsic factors [7]. Efforts to understand why the contribution of MuSC/MPCs to regeneration is reduced in the diseased environment have largely focused on extrinsic signaling factors [8–11]. Less attention has been paid to the

¹Division of Nutritional Sciences, Cornell University, Ithaca, NY, USA ²Department of Bioengineering, University of California San Diego, La Jolla, CA, USA ³Meinig School of Biomedical Engineering, Cornell University, Ithaca, NY, USA ⁴Department of Pediatrics, Division of Neurology at the University of Alabama at Birmingham and Children's of Alabama, Birmingham, AL, USA ⁵UAB Center for Exercise Medicine, Birmingham, AL, USA ⁶Civitan International Research Center at the University of Alabama at Birmingham, Birmingham, AL, USA ⁷Department of Genetics at the University of Alabama at Birmingham, Birmingham, AL, USA ⁸College of Agriculture and Life Sciences, Texas A&M University, College Station, TX, USA ⁹Department of Cell, Developmental and Integrative Biology, University of Alabama at Birmingham, USA

*Corresponding author. Department of Cell, Developmental and Integrative Biology, Lab THT948, 1900 University Blvd., Birmingham, AL, 35294-0066, USA. E-mail: athalack@uab.edu (A.E. Thalacker-Mercer).

Received August 25, 2020 • Revision received October 8, 2020 • Accepted October 21, 2020 • Available online 23 October 2020

<https://doi.org/10.1016/j.molmet.2020.101106>

changing availability of nutrients and their metabolic derivatives, despite documented alterations in the systemic metabolome of older adults and in disease states where muscle regeneration is defective [12–14].

Accelerated proliferation, such as that needed by MuSC/MPCs at the onset of regeneration, has been associated with increased nutrient uptake from cell-extrinsic sources in other cell types [15]. Interestingly, circulating levels of serine and/or glycine, two nutritionally non-essential amino acids, are reduced systemically in human cohorts of aged individuals [16] and those with CKD [17], diabetes [14], and muscle dystrophies [12]. These findings are pertinent as serine is readily interconverted to glycine via a one-step reaction catalyzed by serine hydroxymethyltransferase (SHMT) enzymes, and serine and/or glycine are essential for proliferation in some types of cancer cells [18–20] and T cells [21]. A number of studies have identified glycine supplementation as a therapy for improving skeletal muscle maintenance in various settings, including cancer cachexia [22], muscle dystrophy [23,24], sepsis [25], and calorie restriction [26]. Therefore, we hypothesized that the availability of serine and glycine in MuSC/MPCs during proliferation may dictate MuSC/MPC function and subsequently efficient skeletal muscle regeneration.

In this study, we identified that extracellular serine/glycine is required for the *in vitro* proliferation of human MPCs (*hMPCs*). Further, by using a model of reduced extracellular serine/glycine availability induced via dietary restriction of serine/glycine, we demonstrated that MuSC abundance is reduced 3 days post-injury (dpi) in mice. Subsequent experiments in primary *hMPCs* identified that the capacity of *hMPCs* for *de novo* serine/glycine biosynthesis is limited and, therefore, when they are cultured without extracellular serine/glycine, proliferation halts and *hMPCs* arrest in a G0/G1 state. The requirement for extracellular serine/glycine is attributed in part to the need for glutathione and global protein synthesis. We determined that cell cycle arrest, which occurs in response to serine/glycine restriction, happens in a phospho-EIF2 α (pEIF2 α)-dependent manner. We also build upon prior research that showed a reduction in serine in the circulation of older adults [13] by demonstrating that serine levels in skeletal muscle tissue homogenates are negatively correlated with age. We show that when available serine/glycine is reduced via dietary serine/glycine restriction in old (>20 mo) mice, there is a decrease in MuSC abundance at 3 dpi and increased intramuscular fat deposition at 28 dpi. These results demonstrate that serine and glycine availability is required for skeletal muscle regeneration and augment impaired regeneration in pathological states.

2. METHODS

2.1. Human participants

Younger (21–40 years) and older adults (65–80 years) were recruited from the Tompkins County, New York area. Participants were excluded if they had a history of negative or allergic reactions to local anesthetic, used immunosuppressive medications, were prescribed anti-coagulation therapy, were pregnant, had a musculoskeletal disorder, suffered from alcoholism (>11 drinks per week for women and >14 drinks per week for men) or other drug addictions, or were acutely ill at the time of participation [27,28]. The Cornell University Institutional Review Board approved the protocol and all the subjects provided written informed consent in accordance with the Declaration of Helsinki.

2.2. Human skeletal muscle biopsies

Skeletal muscle tissue was obtained from the vastus lateralis muscle of humans using percutaneous biopsies. Visible connective or

adipose tissues were removed at the time of biopsy. For tissue homogenate experiments, the biopsy sample was measured for wet weight and then snap-frozen in liquid nitrogen and stored at -80°C . For cell culture experiments, a 60–100 mg portion of the tissue was stored in Hibernate-A medium (Invitrogen) at 4°C until tissue disassociation was performed (within 48 h). The demographic characteristics of the biopsy donors can be found in [Supplementary Table 1](#).

2.3. Primary *hMPC* culture

Primary *hMPC* cultures were obtained as previously described [27–30]. Briefly, skeletal muscle tissue stored in Hibernate-A medium (Invitrogen) was minced and washed via gravity with Dulbecco's PBS (Gibco) and then digested using mechanical and enzymatic digestion in low-glucose Dulbecco's Modified Eagle Medium (DMEM, Gibco). This solution was passed through a 70- μm cell strainer into 5 mL of a growth medium comprised of Ham's F12 (Gibco), 20% FBS, 1% penicillin/streptomycin (Corning), and 5 ng/mL of recombinant human basic fibroblast growth factor (bFGF, Promega) and then centrifuged. The pelleted cells were resuspended in growth media containing 10% DMSO and cryopreserved at -80°C until isolation via flow cytometry. Primary *hMPCs* were sorted using fluorescence-activated cell sorting with fluorescently conjugated antibodies to cell surface antigens specific to *hMPCs* (CD56 [NCAM, BD Pharmingen] and CD29 [β 1-integrin, BioLegend]) and a viability stain (7-Aminoactinomycin D, eBioscience) [31]. Passage six *hMPCs* were used for all the experiments and were cultured in a 5% CO_2 atmosphere at 37°C on collagen-coated plates (Type I, rat tail, Corning). For cell culture experiments, donor cells from the same 5 females ([Supplementary Table 2](#)) were used exclusively due to availability of adequate samples as *hMPCs* from male donors have failed to provide adequate yield to conduct the required experiments [27].

hMPCs were initially seeded in the previously described growth medium before being switched to treatment medium 24 h later. For all the experiments, a specially formulated DMEM devoid of serine, glycine, methionine, choline, pyridoxine, glucose, folate, nucleotides, and nucleosides that was supplemented with dialyzed and charcoal-treated FBS (10%), 200 μM of methionine, 4 mg/L of pyridoxine, 5 ng/mL of bFGF, 25 nM of (6S) 5-formylTHF, penicillin-streptomycin (1%), 10 mmol/L of glucose, 4 mM of Glutamax (Gibco), as well as L-serine and glycine in varying concentrations. Unless otherwise noted, all of the assays were conducted after 5 days in the specified treatment medium as this was the time point when differences in cell numbers between cells grown in serine/glycine restricted and replete media were initially identified. Treatments included glutathione ethyl ester (GSHee, Cayman Chemical), L-Buthionine-sulfoximine (Sigma–Aldrich), and ISRIB (Sigma–Aldrich). In all of the experiments, the cell culture media was replenished daily. All the experiments contained appropriate vehicle controls (DMSO or sterile H_2O).

2.4. Mice

The Institutional Animal Care and Use Committee at Cornell University approved all of the animal procedures described. Young female C57BL/6J (4–6 mo) mice were obtained from the Jackson Laboratory and old mice (>20 mo) were acquired from the National Institutes of Aging colony at Charles River. Upon arrival, all the mice were allowed to acclimatize to the new facility for at least one week before being housed at 3–4 mice per cage with Omega-Dry bedding.

2.5. Diet intervention in mice

The mice were randomized to consume either a serine/glycine-containing diet (control) or a serine/glycine-free diet (Ser/Gly_{depleted}) *ad libitum* for 4 weeks prior to injury until sacrifice. Diets were formulated to be isonitrogenous and isoenergetic. The full composition of the diets can be found in [Supplementary Table 3](#) (Dyets Inc.). Weekly throughout the study, food was replaced and food intake was measured at the cage level.

2.6. Body composition assessment of mice

Body weight was measured using a standard laboratory scale, and body composition was measured using nuclear magnetic resonance (NMR, Bruker Minispec LF90II, Bruker) at the indicated time points. NMR was conducted on the live mice to measure their lean and fat mass.

2.7. Skeletal muscle injury and tissue collection in mice

In each mouse, both tibialis anterior (TA) muscles were injected with 10 μ L of notexin under isoflurane anesthesia. The feeding cycle was synchronized to ensure that the metabolite measurements represented long-term effects of the diet rather than recent feeding behaviors. To synchronize the feeding cycle, food was removed from the cage 24 h prior to sacrifice, 12 h later one pellet of food/mouse was provided, and mice were sacrificed 12 h later. One TA muscle per mouse was reserved for histology. For TA muscles used for cryosectioning, the TA was pinned to a cork at resting length, coated with optimal cutting temperature compound (OCT), frozen in liquid-nitrogen-cooled isopentane, and stored at -80°C . Alternatively, TA muscles were fixed in 2% paraformaldehyde (PFA) overnight at 4°C and then stored in EtOH at 4°C prior to paraffin embedding and sectioning. Blood was obtained via cardiac puncture and collected in heparin-coated tubes. Plasma was isolated by centrifugation, frozen in liquid nitrogen, and stored at -80°C ¹⁹.

2.8. Amino acid analysis

Frozen skeletal muscle (20–30 mg) was homogenized using a ball mill (MM 400 Retsch Mixer Mill) at 30 Hz for 3 min in 500 μ L of -20°C methanol, 400 μ L of ice-cold saline, and 100 μ L of ice-cold H_2O containing amino acid isotope-labeled internal standards (#MSK-A2-1.2, Cambridge Isotope Laboratories). Then 50 μ L of the subsequent skeletal muscle homogenate was dried under air and resuspended in radioimmunoprecipitation assay (RIPA) buffer. A bicinchoninic acid assay (BCA, BCA Protein Assay, Lambda Biotech) was used to quantify the total protein levels. The remaining skeletal muscle homogenate was combined with 1 mL of chloroform, vortexed for 5 min, and centrifuged (5 min, 15 000 g, and 4°C). The organic phase was removed, and the polar phase was re-extracted in 1 mL of chloroform. An aliquot of the polar phase was collected, dried under a vacuum at 4°C , and derivatized with 2% (w/v) methoxyamine hydrochloride (Thermo Fisher Scientific) in pyridine for 60 min followed by silylation in *N*-tert-butylidimethylsilyl-*N*-methyltrifluoroacetamide (MTBSTFA) with 1% tert-butylidimethylchlorosilane (tBDMS) (Regis Technologies, Inc.) at 37°C for 30 min. The polar phase was analyzed by gas chromatography (GC)-mass spectrometry (MS) as previously described [32] using a DB-35MS column (30 m \times 0.25 mm i.d. \times 0.25 μ m, Agilent J&W Scientific) installed in an Agilent 7890A GC interfaced with an Agilent 5975C MS.

Three μ L of plasma was spiked with 3 μ L of amino acid isotope-labeled internal standard (Cambridge Isotope Laboratories), extracted with 250 μ L of -20°C methanol for 10 min, and centrifuged at 4°C for 10 min at 15 000 g. Then 200 μ L of supernatant was collected,

vacuum-dried at 4°C , and derivatized with MTBSTFA and tBDMS as prior to analysis similar to that described for skeletal muscle amino acid analysis.

2.9. Histological analysis

To measure the myofiber size, TA sections were stained with hematoxylin and eosin and images were obtained at 10X magnification using a Nikon Eclipse Ti microscope (Nikon). At least 800 myofibers from a minimum of two sections per TA were counted by manually outlining each myofiber using Fiji [33] and the minimum Feret diameter was reported [34].

To determine adipocyte infiltration, paraffin-embedded TA sections were deparaffinized and antigens were retrieved by incubating the sections with a 0.05% trypsin solution at 37°C for 15 min followed by permeabilization by 2×5 min incubations in 0.025% Triton X-100 in TBS. After a 120 min block in 10% goat serum at room temperature (RT), the sections were incubated overnight with perilipin-1 primary antibody (1:100 dilution in TBS with 1% bovine serum albumin, [PERILIPIN-1, Cat: 9349, Cell Signaling Technology]). Perilipin-1 is a cell membrane lipid stain used to visualize adipocytes. Following the overnight incubation in perilipin-1 primary antibody, the sections were washed 2×5 min with 0.025% Triton X-100 in TBS and incubated with a secondary mouse anti-rabbit fluorescent antibody (Alexa Fluor 488 anti-rabbit, Life Technologies) diluted 1:100 in TBS with 1% bovine serum albumin. The sections were then mounted with ProLong Gold mounting medium with DAPI (Thermo Fisher Scientific) and images were obtained at 10X magnification using a Nikon Eclipse Ti microscope (Nikon).

To determine MuSC abundance, cryosectioned TA muscles were fixed with 4% PFA at RT for 7 min followed by 3×3 min washes in PBS. The sections were blocked in 10% goat serum at RT for 60 min before overnight incubation with an anti-laminin antibody diluted to 1:50 in 10% goat serum at 4°C (L9393, MilliporeSigma). The next morning, the sections were washed 3 times for 5 min in PBS and incubated in donkey anti-rabbit IgG Alexa Fluor 647 secondary antibody (A-31573, Thermo Fisher Scientific) diluted to 1:250 in PBS for 60 min at RT. After 2×5 min PBS washes, the sections were placed in sodium citrate antigen-retrieval buffer (10 mM and pH 6.5) at 90°C for 11 min before being allowed to cool to RT. The sections were then washed 3 times for 3 min followed by blocking endogenous peroxidases with 3% H_2O_2 for 7 min at RT and then another set of 3×3 -min PBS washes. A mouse-on-mouse blocking step (1 drop blocking buffer/1 mL PBS, MKB-2213, Vector Laboratories) was conducted for 60 min at RT before a 60 min RT block with 10% goat serum. After incubation overnight at 4°C with Pax7 primary antibody (Pax7 was deposited to the DSHB by A. Kawakami [DSHB Hybridoma Product PAX7]) [35] diluted to 0.5 μ g/mL in 10% goat serum. The next morning, the sections were washed 4 times for 5 min in PBS prior to a 70 min RT incubation with goat anti-mouse biotinylated secondary antibody (115-065-205, Jackson ImmunoResearch Laboratories, Inc.) diluted to 1:1000 in 10% goat serum. To amplify the Pax7 signal, an Alexa Fluor 594 Tyramide SuperBoost Streptavidin Kit was used per the manufacturer's recommendations (B40935, Thermo Fisher Scientific). ProLong Gold mounting medium with DAPI (Thermo Fisher Scientific) was used to mount the sections and images for quantification were obtained at 10X magnification using a Nikon Eclipse Ti microscope (Nikon).

2.10. Live and dead cell counting

The number of live cells was determined by co-staining the cells with Hoechst 33342 (to identify the number of nuclei, Life Technologies) and propidium iodide (to identify dead cells, Thermo Fisher Scientific).

The number of live cells was determined by subtracting the number of propidium iodide-positive cells from the Hoechst 33342-positive cells identified using a Celigo imaging cytometer (Nexcelom).

2.11. RNA isolation and quantification

For quantitative RT-PCR analysis and RNA sequencing (RNA-seq), RNA was isolated from *hMPCs* using an Omega E.Z.N.A. Total RNA Kit I (Omega) according to the manufacturer's instructions. RNA was isolated from human skeletal muscle biopsy tissue using TRIzol Reagent (Ambion) according to the manufacturer's instructions. The amount of RNA was determined spectrophotometrically.

2.12. Quantitative RT-PCR

Gene expression was measured using quantitative RT-PCR. cDNA was synthesized via reverse transcription of extracted RNA using an Applied Biosystems High-Capacity cDNA Reverse Transcription Kit. The TaqMan Gene Expression System (Applied Biosystems) was used to measure mRNA levels of phosphoglycerate dehydrogenase (*PHGDH*, Hs00358823), phosphoserine aminotransferase 1 (*PSAT1*, Hs00268565), and phosphoserine phosphatase (*PSPH*, Hs01921296). All the samples were normalized to *18S* (Hs99999901) expression.

2.13. RNA library preparation and sequencing

Prior to RNA-seq, RNA quality was determined using an AATI Fragment Analyzer; all of the samples had an RNA quality number >8.5. A NEBNext Ultra II RNA Library Prep Kit (New England Biolabs) was used to generate TruSeq-barcoded RNA-seq libraries. The libraries were quantified with Qubit 2.0 (dsDNA HS kit, Thermo Fisher Scientific) and the size distribution was measured with a Fragment Analyzer (Advanced Analytical) before pooling. NextSeq500 (Illumina) was used for sequencing, and a minimum of 20 M of single-end 75 bp reads per library were obtained. Cutadapt v1.8 was used to trim low-quality reads and adaptor sequences (parameters: m 50-q 20-a AGATCGGAAGAGCACACGTCTGAACTCCAG-match-read-wild cards) [36]. TopHat v2.1 was used to map reads to the reference genome (parameters: library-type=fr-firststrandon-no-novel-juncs-G < ref_genes.gtf>) [37]. Differential gene expression analysis was conducted using edgeR [38]. Only genes with at least 2 counts per million in at least three of the samples were retained for analysis.

2.14. Immunoblotting analysis

For immunoblotting analysis, protein was isolated from *hMPCs* with RIPA buffer containing phosphatase (PhosSTOP, Roche) and protease (cOmplete, Roche) inhibitors. The protein concentration was quantified by BCA. Then 8–15 µg of protein was loaded on 10% SDS gels and transferred to PVDF membranes. The membranes were incubated in primary antibodies PHGDH (14719, Proteintech), PSAT1 (10501, Proteintech), PSPH (14513, Proteintech), SHMT1 (Stover Laboratory) [39], SHMT2 (Stover Laboratory) [40], MyoD (sc-304, Santa Cruz), ATF4 (11815, Cell Signaling), phosphorylated (Ser51) p-EIF2α (3398, Cell Signaling), and total EIF2α (5324, Cell Signaling) diluted (1:1000) in a chemiluminescent blocking buffer (block-CH, Millipore) or myogenin (F5D was deposited to the DSHB by W.E. Wright [DSHB Hybridoma Product F5D]) [41] and Pax7 (Pax7 was deposited to the DSHB by A. Kawakami [DSHB Hybridoma Product PAX7]) [35] cell culture supernatant overnight at 4 °C. After overnight incubation, the membranes were washed with 0.1% Tween in tris-buffered saline before incubation with appropriate secondary antibody (rabbit, Proteintech; goat, Thermo Fisher Scientific; mouse, Proteintech; and goat, Pierce) at a 1:100000 dilution in a chemiluminescent blocking buffer at RT for 60 min. The membranes were visualized after brief incubation in

SuperSignal West Femto (Thermo Fisher Scientific) on a Bio-Rad ChemiDoc MP. Protein expression was normalized to α-TUBULIN expression (9099, Cell Signaling) using ImageLab 4.1 software (Bio-Rad).

2.15. Cell cycle analysis

For cell cycle analysis, *hMPCs* were pelleted, washed with ice-cold PBS, re-pelleted and resuspended in PBS, and then fixed in 3:1 volume:volume 100% ice-cold ethanol before being stored at 4 °C overnight. The following day, the cells were pelleted, washed with ice-cold PBS, and resuspended in 400 µL PBS containing 2 mM of EDTA. The cell suspensions were incubated with 100 µL of 10 mg/mL RNase A (VWR) for 30 min at 37 °C to degrade RNA followed by DNA staining with 50 µL of 1 mg/mL propidium iodide for 30 min in the dark at RT. The propidium iodide intensity was measured using a flow cytometer (BD FACSAria Fusion). The percentage of the total population of cells in 2N, S-phase, or 4N were determined using FlowJo's (Becton, Dickinson and Company) univariate platform.

2.16. 5-bromo-2'-deoxyuridine (BrdU) incorporation

To determine the proportion of cells actively synthesizing DNA, *hMPCs* were pulsed with BrdU for 24 h. *hMPCs* were washed with prewarmed PBS before being fixed in ice-cold methanol for 5 min. The cells were washed with PBS before 30 min of acid hydrolysis and cell permeabilization in 2 N HCl prepared in 0.1% PBS-Tween20. The cells were washed with PBS before being blocked in 1% BSA/10% normal goat serum/0.3 M glycine/0.1% PBS-Tween20 followed by washing in PBS. Fixed and blocked *hMPCs* were incubated overnight at 4 °C with an anti-BrdU antibody (1:400 dilution, 317902, BioLegend) followed by PBS washes and a 60 min incubation with an Alexa-Fluor 488 conjugated anti-mouse secondary antibody (Invitrogen). Finally, *hMPCs* were washed with PBS and incubated with Hoechst 33342 before visualization and analysis using a Celigo imaging cytometer (Nexcelom).

2.17. Glucose uptake

Glucose uptake was measured based on the detection of 2-deoxyglucose-6-phosphate uptake using a commercially available luminescence-based kit (Glucose Uptake Glo Assay, Promega) on a SpectraMax M3 (Molecular Devices). Values were normalized to the total cell count obtained from a parallel plate.

2.18. Stable isotope labeling, metabolite extraction, and GC–MS analysis

For isotopic labeling experiments, cells were cultured in 10 mM [U-¹³C₆]glucose (Cambridge Isotope Laboratories, Inc.) containing either 1000 µM of serine/glycine or no serine/glycine for 48 h prior to extraction. A medium exchange was conducted after 24 h. On the extraction day, polar metabolites were extracted as previously described [42].

The upper aqueous phase was derivatized using a Gerstel MPS with 15 µL of 2% (w/v) methoxyamine hydrochloride (Thermo Fisher Scientific) in pyridine (incubated for 60 min at 45 °C) followed by 15 µL of MTBSTFA with 1% tert-butyltrimethylchlorosilane (Regis Technologies) (incubated for 30 min at 45 °C). Polar derivatives were analyzed by GC–MS using a DB-35MS column (30 m × 0.25 mm i.d. × 0.25 µm) installed in an Agilent 7890B GC interfaced with an Agilent 5977B MS with an XTR EI source using the following temperature program: 100 °C initial, increased by 3.5 °C/min to 255 °C, increased by 15 °C/min to 320 °C, and held for 3 min.

2.19. Glutathione measurements

Total and oxidized (GSSG) glutathione were measured using a commercially available luminescence-based kit (GSH-GSSG Glo Assay, Promega) on a SpectraMax M3 (Molecular Devices). The reduced glutathione (GSH) to GSSG ratio was determined by multiplying the GSSG reading by 2 to account for each mole of oxidized GSSG producing two moles of total glutathione, subtracting that number from the total glutathione levels, and then dividing this value by the total GSSG reading. Values were normalized to the total cell count obtained from a parallel plate.

2.20. Reactive oxygen species (ROS) detection

To determine the intracellular level of ROS, *hMPCs* were pelleted and resuspended in 1 mL of pre-warmed PBS with CellROX Green Reagent (Invitrogen), a cell-permeable dye that fluoresces green and binds to DNA upon oxidation at a final concentration of 5 μM . After a 30 min incubation at 37 $^{\circ}\text{C}$, *hMPCs* were washed with PBS before being fixed in 2% paraformaldehyde for 10 min at room temperature. *hMPCs* were again washed with PBS before finally being resuspended in 300 μL of 0.5 mM EDTA in PBS and analyzed via flow cytometry (BD FACSAria Fusion).

2.21. Protein synthesis

2.21.1. O-propargyl-puromycin incorporation

To determine protein synthesis, a commercially available fluorescence-based kit was used (Click-iT Plus OPP Alexa Fluor 488 Protein Synthesis Assay Kit, Invitrogen) according to the manufacturer's directions. The integrated intensity of fluorescent signals within the nuclei was quantified using a Celigo imaging cytometer (Nexcelom).

2.21.2. SUnSET method

The SUnSET method [43] was used to quantify the rate of puromycin incorporation to approximate protein synthesis [44]. *hMPCs* were treated with 0.5 $\mu\text{g}/\text{mL}$ of puromycin (Thermo Fisher Scientific) for 30 min and immediately harvested in RIPA buffer and the protein was isolated as previously described. Immunoblotting was conducted as described using a primary antibody specific for puromycin (MABE343, Millipore) diluted 1:1000 in a chemiluminescent blocking buffer overnight prior to incubation in secondary antibody (mouse, Proteintech) diluted to 1:100000. Membranes were incubated in Super-Signal West Femto (Thermo Fisher Scientific) and imaged on a Bio-Rad ChemiDoc MP. The puromycin expression was normalized to the total protein level in each respective lane as determined by Coomassie staining and imaging on a Bio-Rad ChemiDoc MP using ImageLab 4.1 software (Bio-Rad).

2.22. Statistics

Statistical analyses were performed in R Studio (Version 1.0.136). For metabolite analysis of the whole skeletal muscle tissue, the normalcy of the distribution of each amino acid was assessed by the Shapiro–Wilk test. If the data were determined to be normally distributed, they were compared via an unpaired t-test; otherwise, they were compared by the Mann–Whitney U-test. The correlation between skeletal muscle serine levels and age was determined using Pearson's correlation coefficient. An unpaired t-test was used for body composition, metabolite analyses, myofiber size, and Pax7⁺ cell frequency. For cell counting experiments, two-way ANOVA was conducted with time and treatment being the main factors. Tukey's *post hoc* test was performed if the interaction term was significant ($p < 0.05$). For all the *hMPC* assays, either a paired t-test or a repeated measures ANOVA was employed.

3. RESULTS

3.1. *hMPCs* required extracellular serine/glycine for population expansion

We first evaluated whether serine and glycine alone or in combination impact *hMPC* population expansion. When *hMPCs* were cultured without serine and glycine, they did not undergo population expansion (Figure 1A). The addition of serine (Figure S1A) and glycine (Figure S1B) individually or in combination (Figure 1A) increased *hMPC* population expansion in a dose-dependent manner. At high doses, glycine alone was more effective at increasing *hMPC* population expansion than serine (Figure S1C). This finding is dissimilar to that observed in other non-muscle cell types in which serine but not glycine is more potent for increasing population expansion [18,20,21]. We verified that extracellular serine/glycine restriction reduced intracellular serine and glycine levels (Figure 1B), demonstrating that extracellular serine/glycine availability dictated the intracellular serine/glycine levels in *hMPCs*.

To determine the physiological relevance of the serine and glycine concentrations used *in vitro*, we measured plasma serine and glycine concentrations from a cohort of human adults under fasted and resting conditions. The levels of plasma serine ranged between 76 and 212 $\mu\text{mol}/\text{L}$ and plasma glycine ranged between 178 and 632 $\mu\text{mol}/\text{L}$ (Figure 1C). However, the levels of these amino acids in circulation are frequently elevated above basal values in the non-fasted state [45,46]. Additionally, serine/glycine availability to MuSC/MPCs from the skeletal muscle is potentially higher than concentrations observed in the circulation. Bergström et al. demonstrated that in younger adults, skeletal muscle concentrations of serine and glycine are ~ 980 $\mu\text{mol}/\text{L}$ and ~ 1330 $\mu\text{mol}/\text{L}$, respectively, > 3.5 fold higher than observed in plasma [47].

3.2. Serine and glycine availability impacted MuSC abundance after skeletal muscle injury

To understand the effect of available serine/glycine *in vivo* on MuSC abundance after skeletal muscle injury, the mice were randomized to consume isocaloric, isonitrogenous diets either containing (control) or not containing serine/glycine (Ser/Gly_{depleted}). The animals consumed the respective diets for four weeks prior to and after notexin-induced skeletal muscle injury (Figure 1D). After four weeks of the Ser/Gly_{depleted} diet compared to the control diet, skeletal muscle levels of serine prior to injury decreased by 38% and 42% in the skeletal muscle and plasma, respectively, with a less consistent effect on glycine levels (Figure 1EF). The mice fed the Ser/Gly_{depleted} diet had reduced numbers of MuSCs at 3 dpi indicating that the abundance of MuSCs after injury was heavily influenced by serine/glycine availability *in vivo* (Figure 1GH).

3.3. *hMPCs* exhibited limited capacity for *de novo* serine/glycine biosynthesis

We hypothesized that *hMPCs* lack the ability for *de novo* serine/glycine biosynthesis, which would underlie the extracellular requirement for these amino acids when *hMPCs* are cultured *in vitro*. In contrast to this hypothesis, RNA-seq analysis revealed that *hMPCs* drastically upregulated serine/glycine biosynthesis genes in response to serine/glycine restriction (Figure 2A and Supplementary Table 4). We further verified that the serine/glycine biosynthesis enzymes (PHGDH, PSPH, PSAT1, SHMT1, and SHMT2) were expressed at the protein level and most were upregulated in response to serine/glycine restriction (Figure 2B). The serine synthesis pathway branches from glycolysis at 3-phosphoglycerate using glucose as the initial substrate (Figure 2E);

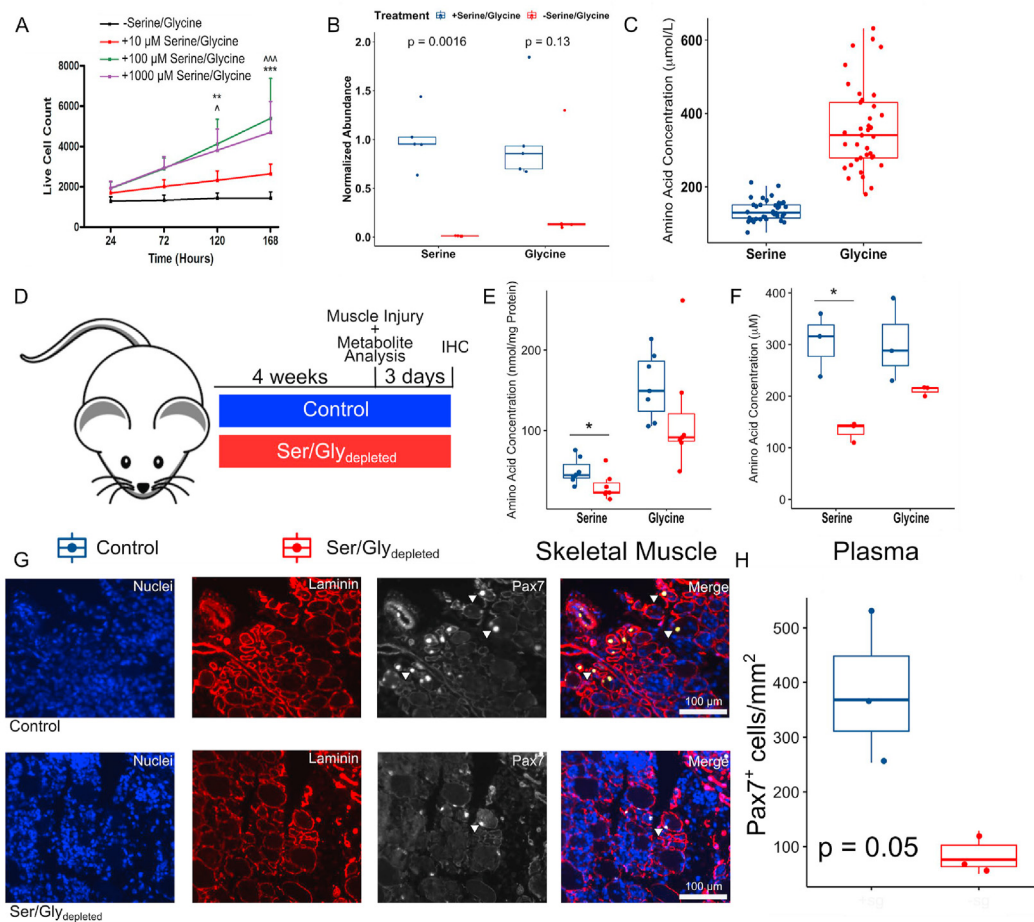


Figure 1: Serine/glycine availability impacted *hMPC* population expansion *in vitro* and mouse MuSC abundance *in vivo*.

A) Live cell count was determined by co-staining cells with Hoechst 33342 (to identify all of the cells) and propidium iodide (to identify dead cells) after *hMPCs* were cultured in media lacking serine/glycine or increasing concentrations of serine/glycine (**indicates significant difference between 100 μM vs -serine/glycine, $p < 0.01$, ***indicates significant difference between 100 μM vs -serine/glycine, $p < 0.001$, *indicates significant difference between 1000 μM vs -serine/glycine, $p < 0.05$, **** indicates significant difference between 1000 μM vs -serine/glycine, and $p < 0.001$).

B) Levels of serine and glycine in *hMPCs* after 7 days of culture in serine/glycine restricted media as determined by GC-MS.

C) Levels of serine and glycine in the plasma of fasted young humans ($n = 37$) based on GC-MS measurements.

D) Schematic of dietary intervention and skeletal muscle injury design as well as subsequent analysis. IHC, immunohistochemistry.

E) Serine and glycine concentrations in skeletal muscle tissue after 4 weeks of the control or Ser/Gly_{depleted} diet in mice (4–6 mo) as measured by GC-MS ($n = 3$ –7 per group).

F) Serine and glycine concentrations in plasma after 4 weeks of the control or Ser/Gly_{depleted} diet in mice (4–6 mo) as measured by GC-MS ($n = 3$ –6 per group).

G) Representative images of cross-sections of TA muscles at 3 dpi in mice (4–6 mo) fed either the control or Ser/Gly_{depleted} diet stained for DAPI (blue), laminin (red), and Pax7 (white). White arrows identify Pax7⁺ staining.

H) Quantification of number of Pax7⁺ cells in cross-sections of injured TA muscles 3 dpi in mice (4–6 mo) fed either the control or Ser/Gly_{depleted} diet ($n = 3$ per group).

All the experiments were repeated with *hMPCs* derived from the same 5 donors. P values or marks of significance are indicated in the appropriate graphs.

however, glucose uptake did not increase after serine/glycine restriction (Figure 2C). Further, increasing glucose concentrations in the media did not affect *hMPC* proliferation in the absence of serine/glycine (Figure 2D), which suggested a limited capacity for serine/glycine biosynthesis by *hMPCs*. Using stable isotope tracing with ¹³C₆ glucose, we determined that *de novo* biosynthesis accounted for no detectable intracellular serine and glycine when serine and glycine were available in the media (Figure 2E). During extracellular serine/glycine restriction, *de novo* biosynthesis contributed ~25% of serine and ~5% of glycine to the intracellular pools (Figure 2E), demonstrating that *hMPCs* have the capacity for serine/glycine biosynthesis under restricted conditions. However, the increase in *de novo* biosynthesis was ineffective to maintain the requirements for proliferation or the intracellular levels of serine and glycine (Figure 1AB).

3.4. Extracellular serine/glycine restriction caused cell cycle arrest in G0/G1 in *hMPCs*

We next sought to understand what drives the reduction in *hMPC* population expansion in the absence of extracellular serine/glycine availability. We observed no differences in the percent of dead cells during *hMPC* population expansion (Figure 3A), demonstrating that differences in cell number were not explained by an effect of serine/glycine restriction on the cell death rate. Using DNA staining and analysis via flow cytometry, we observed a higher number of cells in the early phases of the cell cycle with serine/glycine restriction (Figure 3B). Similarly, a smaller proportion of *hMPCs* cultured in a serine/glycine restricted media incorporated BrdU into DNA after a 24-h BrdU pulse (Figure 3C), indicating that *hMPCs* were arrested in G0/G1. Because *hMPC* differentiation is modeled *in vitro* by restriction of

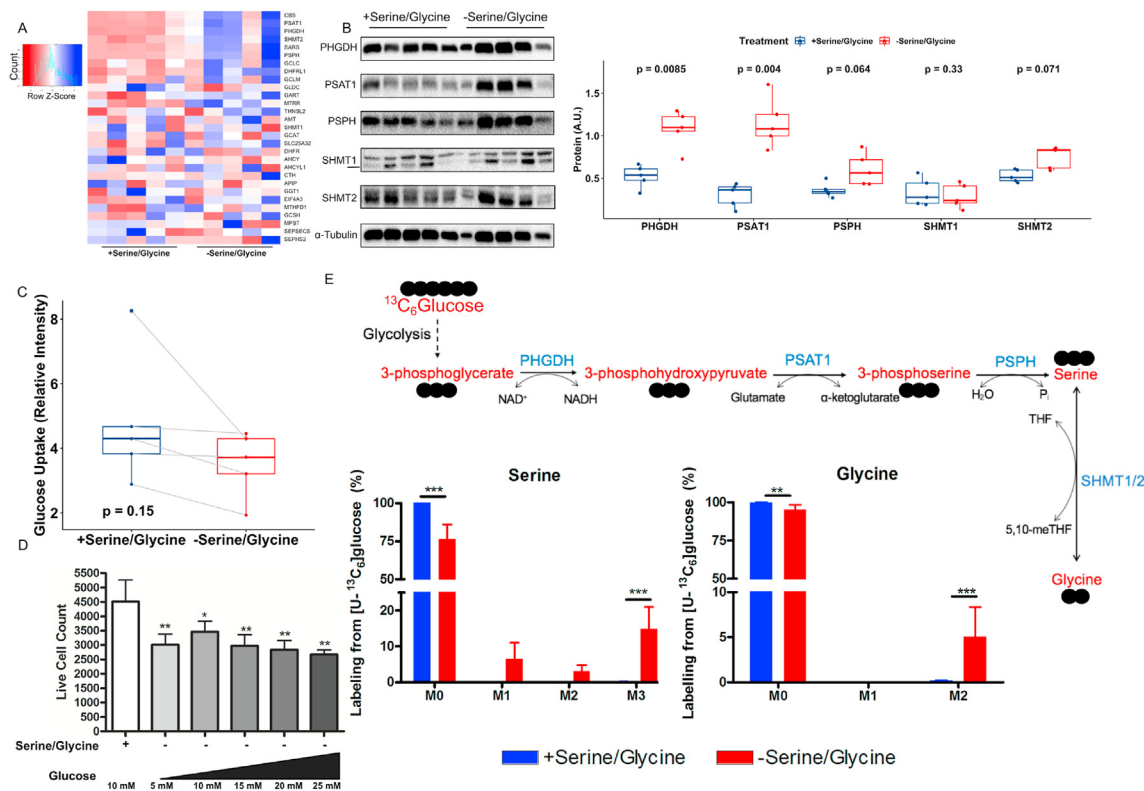


Figure 2: *hMPCs* exhibited limited capacity for serine/glycine biosynthesis.

A) Heatmap of genes involved in serine, glycine, and one-carbon metabolism based on RNA-seq data from *hMPCs* after 5 days of culture in serine/glycine replete (1000 μM) or restricted conditions.

B) Immunoblot for PHGDH, PSAT1, PSPH, SHMT1, and SHMT2 protein normalized to α -TUBULIN for quantification in *hMPCs* that had been serine/glycine restricted for 5 days.

C) Glucose uptake by *hMPCs* after 5 days of culture in serine/glycine replete or restricted conditions.

D) Live cell count of *hMPCs* cultured in serine/glycine replete media or serine/glycine restricted media and varying doses of glucose. * $p < 0.05$ and ** $p < 0.01$ relative to serine/glycine containing control. Data are expressed as mean \pm SD.

E) Percent mass isotopomer distribution of [U-¹³C₆]-glucose-derived serine and glycine in *hMPCs* cultured in serine/glycine replete (1000 μM) or restricted media for 5 days followed by 48 h in similar media but containing [U-¹³C₆]-glucose. Data are expressed as mean \pm SD. ** $p < 0.01$ and *** $p < 0.001$.

All the experiments were repeated with *hMPCs* derived from the same 5 donors. P values or marks of significance are indicated in the appropriate graphs.

serum [48], a key source of nutrients including amino acids, we measured the *hMPC*-specific mid-to-late differentiation marker MYOGENIN, which was undetectable (Figure 3D). Furthermore, *hMPCs* that had been serine/glycine restricted for 7 days maintained their population expansion potential (Figure 3E), suggesting that serine/glycine restriction does not induce terminal differentiation. Additionally, we measured the levels of *hMPC*-specific transcription factors PAX7 and MYOD within a PAX7⁺ population using purified *hMPCs* and found that both transcription factors were significantly elevated in serine/glycine restricted conditions (Figure 3D). Elevated MYOD levels in the *hMPC* population further support cell cycle arrest in G1; MYOD protein levels typically increase in *hMPCs* during G1 of the cell cycle [49].

Serine and glycine are two primary sources of cellular one-carbon units. Both are metabolized to formate by mitochondrial folate metabolism, and formate then serves as the primary one-carbon unit to support cytosolic and nuclear one-carbon metabolism (synthesis of purines, thymidine, and methionine to support cellular methylation reactions) [50,51]. In previous studies, proliferative cell types demonstrated an extracellular requirement for serine/glycine that was attributed to one-carbon metabolism [18,21]. In these prior studies, serine depletion in the presence/absence of glycine was rescued by the addition of formate. In contrast, in *hMPCs*, the serine/glycine

requirement goes beyond one-carbon metabolism and the generation of nucleotides, as supplementation with formate (Figure S2A) or nucleotide precursors did not rescue *hMPC* population expansion (Figure S2B).

3.5. Extracellular serine/glycine restriction depleted intracellular glutathione and promoted elevated ROS in *hMPCs*

Several genes related to glutathione biosynthesis were upregulated in the transcriptomic dataset with serine/glycine restriction (Figures 2A, Figure 4A, and Supplementary Table 2). Because glycine is one of the three amino acids that comprise the tripeptide glutathione (that is, glycine, glutamate, and cysteine) and serine can be metabolized to cysteine, we hypothesized that serine/glycine restriction reduced glutathione levels in *hMPCs* and impaired population expansion. Serine/glycine restriction in *hMPCs* decreased total glutathione levels by 9-fold (Figure 4B) and decreased the ratio of reduced (GSH):oxidized (GSSG) glutathione (Figure 4C). As would be expected with lower glutathione levels, the primary intracellular antioxidant, we observed an increase in the levels of ROS (Figures 4D). Supplementation with a cell permeable version of glutathione, GSHee, modestly increased intracellular glutathione levels (Figure 4E) and decreased ROS levels (Figure 4F). Despite only a modest effect on intracellular glutathione

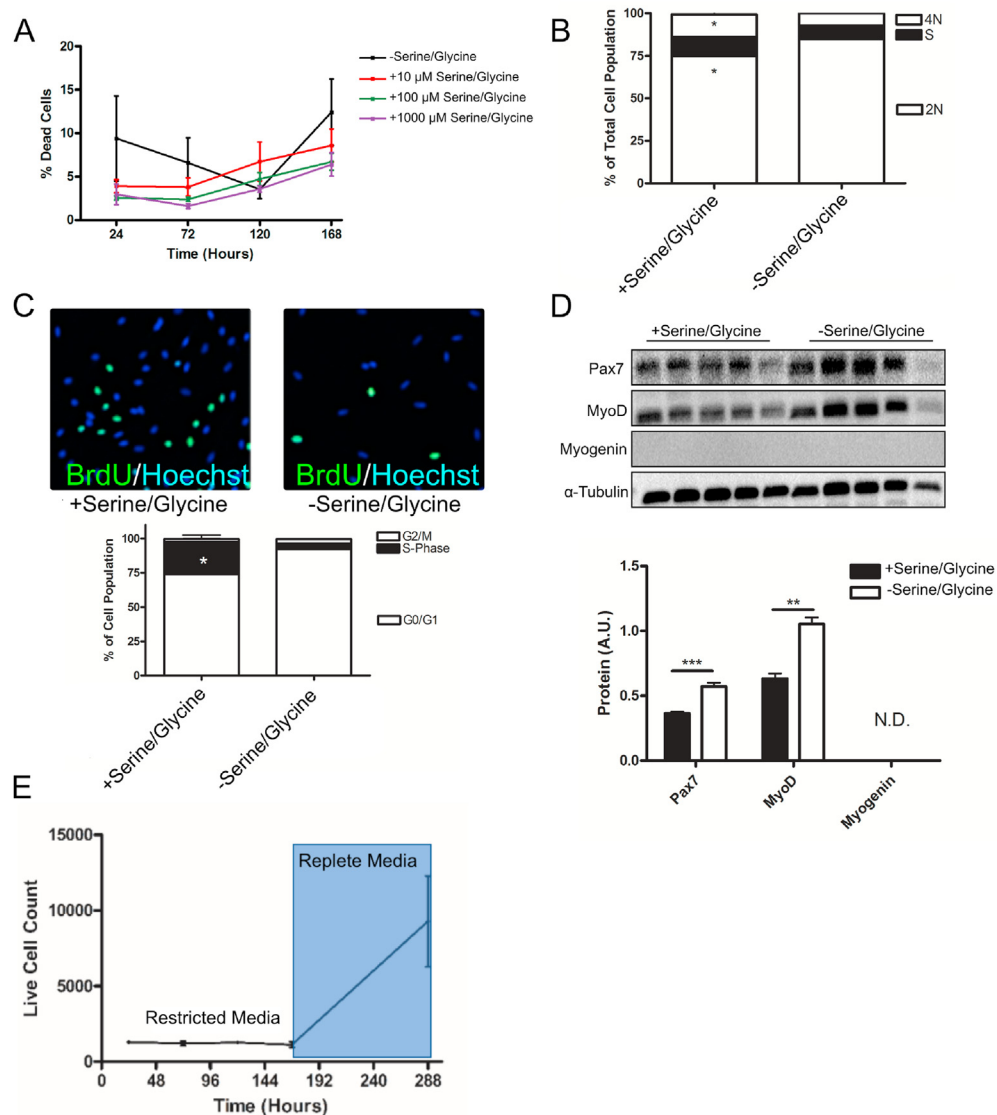


Figure 3: Serine/glycine restriction caused cell cycle arrest in *hMPCs*.

A) Percentage of dead cells was quantified by dividing all the *hMPCs* that stained positive for propidium iodide by all of the *hMPCs* that stained positive for Hoechst 33342 after 5 days of culture in media with varying concentrations of serine/glycine.

B) Propidium iodide staining and analysis via flow cytometry was used to determine the DNA content of *hMPCs* after 5 days of serine/glycine restriction. * $p < 0.05$.

C) BrdU incorporation after a 24-h pulse in *hMPCs* undergoing serine/glycine restriction for 5 days. Data are expressed as mean \pm SD.

D) Immunoblot for PAX7, MYOD, and MYOGENIN protein normalized to α -TUBULIN for quantification in *hMPCs* that had been serine/glycine restricted for 5 days. ** $p < 0.01$ and *** $p < 0.001$. N.D., not detectable. Data are expressed as mean \pm SD.

E) The number of live cells after culture in serine/glycine restricted followed by serine/glycine replete media.

All the experiments were repeated with *hMPCs* derived from the same 5 donors.

levels, GSHee did provide a minor rescue to *hMPC* population expansion (Figure 4G). Of note, high levels of GSHee were toxic to *hMPCs* (Figure S3A) and therefore we could not investigate a GSHee dose that increased intracellular levels of glutathione to that observed in *hMPCs* cultured in serine/glycine replete conditions. We further demonstrated that inhibition of glutathione synthesis with L-buthionine sulfoximine (GSHi) in the presence of serine/glycine resulted in similar total glutathione levels in *hMPCs* as those cultured in serine/glycine restricted conditions (Figure 4H). Similarly, GSHi in the presence of serine/glycine reduced *hMPC* population expansion to a similar extent as serine/glycine restriction (Figure 4I), an effect that was independent

of increased cell death (Figure S3B). We propose that ROS associated with *hMPC* proliferation cannot be counterbalanced during serine/glycine restriction due to reduced glutathione synthesis caused by limited serine/glycine availability, ultimately leading to cell cycle arrest.

3.6. Serine/glycine restriction suppressed global protein synthesis and *hMPC* proliferation

Serine/glycine biosynthetic genes are targets of activating transcription factor 4 (ATF4), a transcription factor selectively translated as a part of the integration of cellular stress signals (that is, the integrated stress response), including nutrient limitations [52]. We hypothesized that

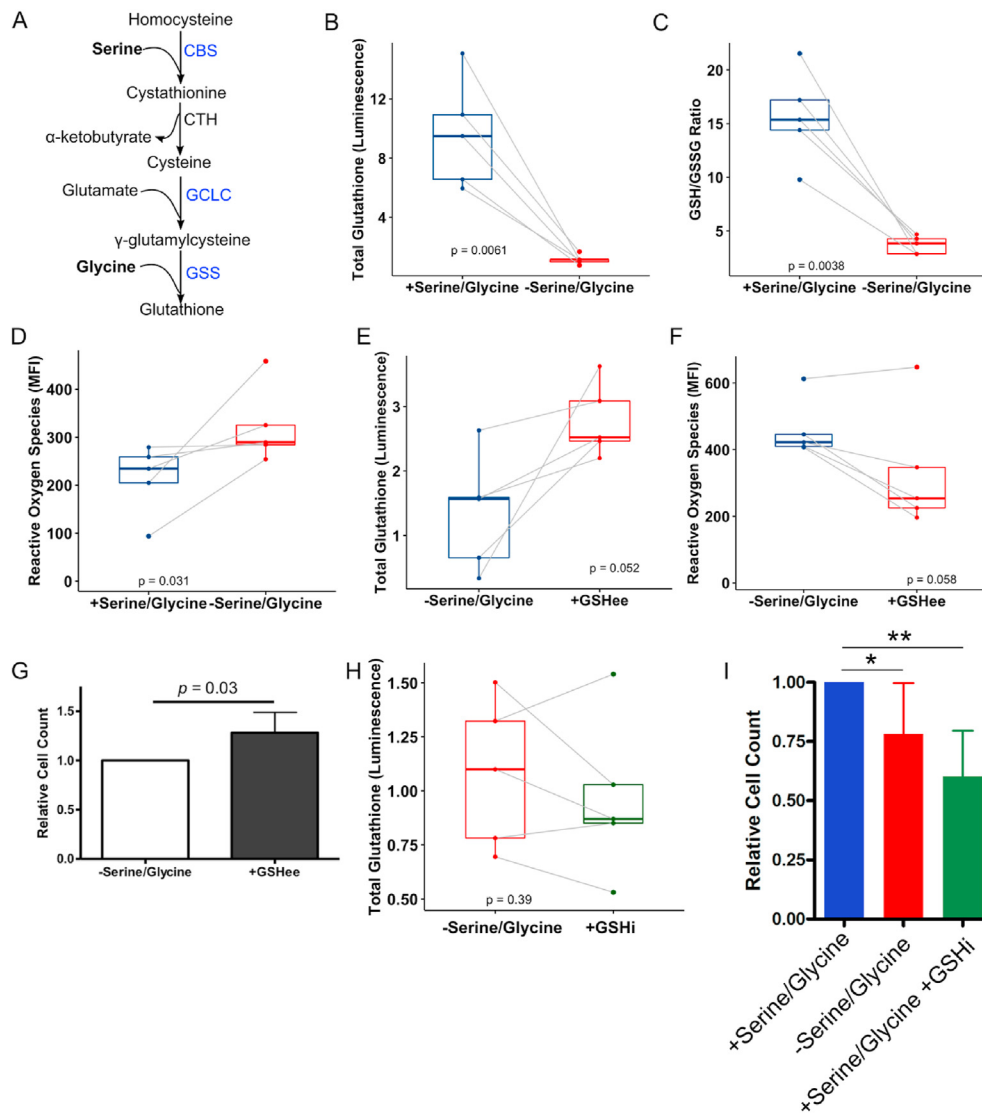


Figure 4: Serine/glycine restriction reduced intracellular glutathione levels that are necessary for *hMPC* proliferation.

A) The glutathione synthesis pathway with genes upregulated after serine/glycine restriction according to RNA-seq is in blue. CBS, cystathionine β-synthase; CTH, cystathionine gamma-lyase; GCLC, glutamate-cysteine ligase catalytic subunit; GSS, glutathione synthetase.

B) Total intracellular glutathione levels in *hMPCs* after 5 days in serine/glycine restricted or replete media.

C) Ratio of reduced to oxidized intracellular glutathione levels in *hMPCs* after 5 days in serine/glycine restricted or replete media. GSH, reduced glutathione; GSSG, oxidized glutathione.

D) ROS in *hMPCs* after 5 days in serine/glycine restricted or replete media.

E) Total intracellular glutathione levels in *hMPCs* after 5 days of serine/glycine restriction with or without 10 μM of cell permeable glutathione ethyl ester (GSHee).

F) ROS in *hMPCs* after 5 days of serine/glycine restriction with or without 10 μM of GSHee.

G) Live cell count after 5 days of serine/glycine restriction with or without GSHee (10 μM).

H) Total intracellular glutathione levels in *hMPCs* after 5 days of serine/glycine restriction or 1000 μM of serine/glycine and 100 μM of glutathione inhibitor L-buthionine sulfoximine (GSHi).

I) Live cell count after 5 days of *hMPCs* cultured in serine/glycine replete media, serine/glycine restricted media, or a combination of serine/glycine replete media and 100 μM of GSHi. * $p < 0.05$ and ** $p < 0.01$.

All the experiments were repeated with *hMPCs* derived from the same 5 donors. P values or marks of significance are indicated in the appropriate graphs.

ATF4 translation was triggered by limited serine/glycine availability, producing a transcriptional response (Figure 2A). In the RNA-seq dataset obtained from *hMPCs* under serine/glycine replete and restricted conditions (Supplementary Table 1), we noted several ATF4 target genes (55/57) that were significantly affected by serine/glycine restriction (Figure 5A). ATF4 mRNA is selectively translated in a p-eIF2α-dependent manner. We verified that the protein levels of both

ATF4 and p-eIF2α increased after serine/glycine restriction (Figure 5B). Phosphorylation of eIF2α is known to coordinate a global decline in protein synthesis [53] and cell proliferation [54]. In support of this, in *hMPCs* cultured in the absence of serine/glycine, we observed an accumulation of most of the free non-serine/glycine amino acids (Figure 5C) and a reduction in total protein synthesis (Figure 5D and Figure S4A).

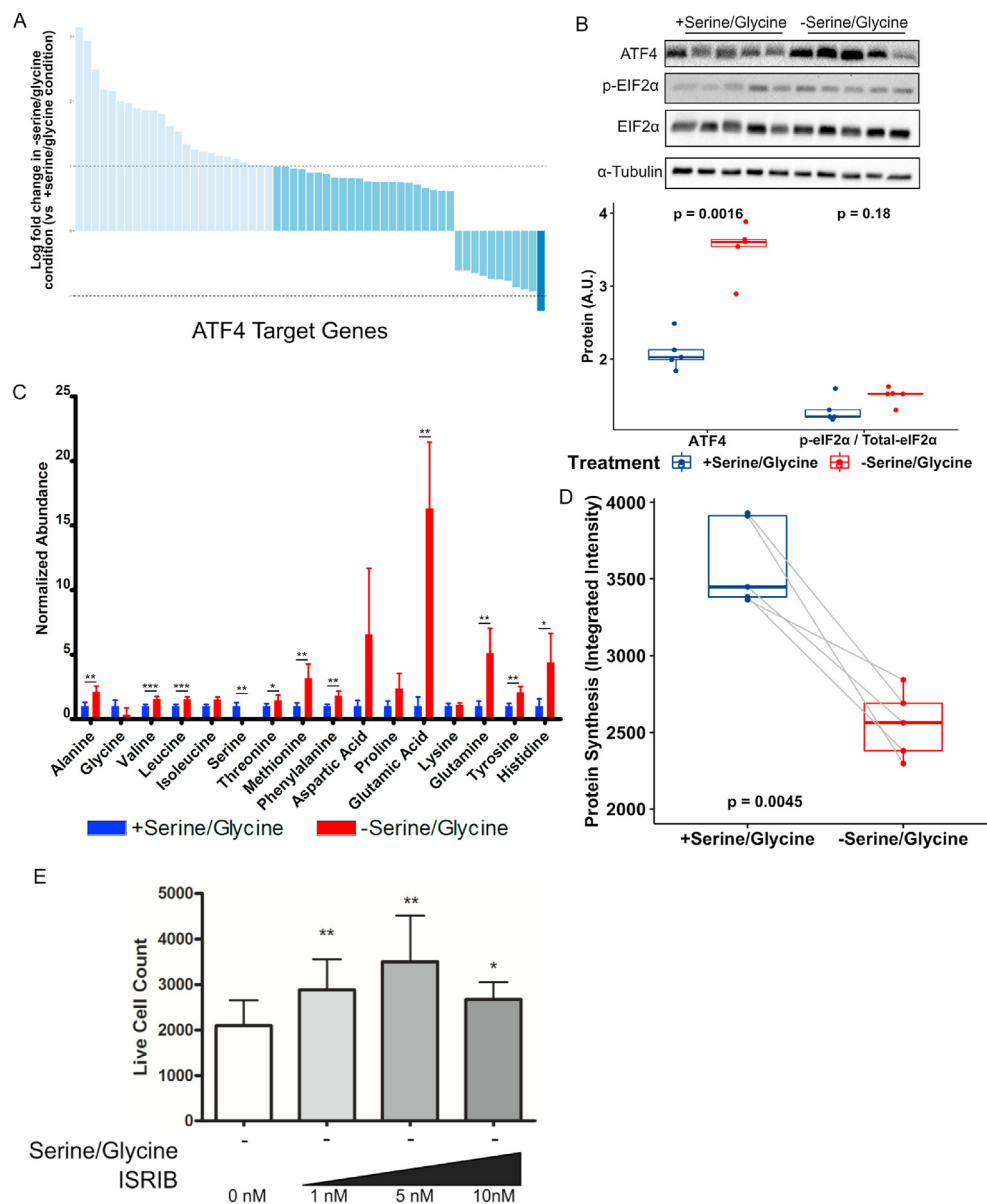


Figure 5: Serine/glycine restriction depressed global protein synthesis and *hMPC* proliferation in a p-eIF2 α -dependent manner.

A) Expression of known ATF4 targets based on RNA sequencing of *hMPCs* cultured in serine/glycine restricted media or serine/glycine replete media for 5 days. Average log fold change of transcripts in serine/glycine restricted samples vs serine/glycine replete samples. Dark blue indicates log fold change < -1 and light blue indicates log fold change > 1.

B) Top, protein levels of ATF4, p-eIF2 α , and total eIF2 α determined by immunoblot *hMPCs* cultured in serine/glycine replete or restricted media. Expression was initially normalized to α -TUBULIN expression and p-eIF2 α normalized to total eIF2 α expression. Bottom, quantification of protein expression.

C) Intracellular amino acid abundance normalized to the total ion count in *hMPCs* cultured in serine/glycine replete or restricted media for 5 days.

D) Protein synthesis as determined by O-propargyl-puromycin incorporation of *hMPCs* cultured in serine/glycine replete or restricted media.

E) Live cell count after 5 days of serine/glycine restriction with or without varying doses of ISRIB. * $p < 0.05$ and ** $p < 0.01$.

All the experiments were repeated with *hMPCs* derived from the same 5 donors. P values are indicated in the appropriate graphs.

To directly test whether the p-eIF2 α response was responsible for arrest of *hMPC* proliferation, *hMPCs* were cultured with ISRIB, a small molecule that reverses the effect of p-eIF2 α [55]. Treatment with ISRIB increased the number of *hMPCs* in the absence of serine/glycine (Figure 5E). Interestingly, ISRIB treatment in the presence of serine/glycine negatively affected the cell number (Figure S5A), suggesting that the benefit of abrogating the effect of p-eIF2 α signaling on *hMPC* proliferation only occurred when aberrant mRNA translation was induced by serine/glycine restriction.

3.7. Serine/glycine availability impacted skeletal muscle regeneration in old mice

Systemic serine and/or glycine levels are reduced in various pathologies and with advanced age [12–14,16,17], and these conditions are also associated with impaired skeletal muscle regeneration [2–6]. Using skeletal muscle biopsy tissue of healthy older and younger adults, we identified serine as the only measured amino acid that was reduced in the skeletal muscle with age in our human cohort (Figure 6A and Figure S6A); a similar analysis in young and old mice on

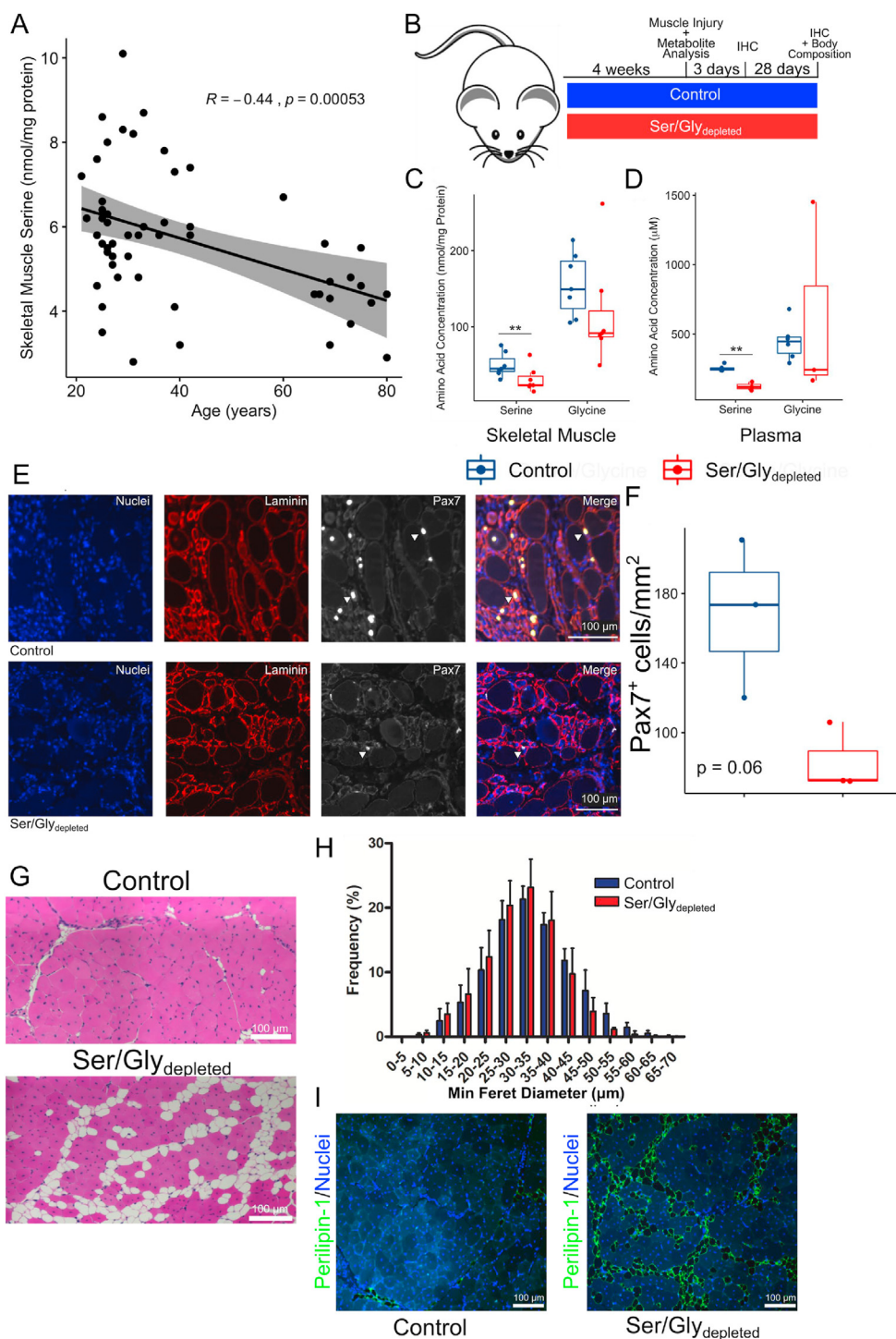


Figure 6: Dietary restriction of serine/glycine disrupted cell numbers and impaired muscle regeneration in the aged mice.

A) Skeletal muscle serine levels negatively correlated with age ($n = 58$, $r = -0.44$, and $p < 0.0001$) based on Pearson's correlation coefficient.

B) Schematic of dietary intervention and skeletal muscle injury design as well as subsequent analysis. IHC, immunohistochemistry.

C) Serine and glycine concentrations in skeletal muscle tissue after 4 weeks of the control or Ser/Gly_{depleted} diet in the mice (>20 mo) as measured by GC-MS ($n = 3-7$ per group).

D) Serine and glycine concentrations in plasma after 4 weeks of the control or Ser/Gly_{depleted} diet in the mice (>20 mo) as measured by GC-MS ($n = 3-7$ per group).

E) Representative images of cross-sections of TA muscles at 3 dpi in the mice (>20 mo) fed either the control or Ser/Gly_{depleted} diet stained for DAPI (blue), laminin (red), and Pax7 (white). White arrows identify Pax7⁺ staining.

F) Quantification of the number of Pax7⁺ cells in cross-sections of injured TA muscles at 3 dpi in the mice (>20 mo) fed either the control or Ser/Gly_{depleted} diet ($n = 3$ per group).

G) Representative images of hematoxylin and eosin (H & E) stained TA muscles at 28 dpi in the old mice fed the control or Ser/Gly_{depleted} diet.

H) Quantification of the distribution of myofiber size of TA muscles at 28 dpi in the old mice fed the control or Ser/Gly_{depleted} diet ($n = 3$ per group).

I) Representative images of cross-sections of TA muscles at 28 dpi in the old mice fed either the control or Ser/Gly_{depleted} diet stained for DAPI (blue) and perilipin-1 (green).

an amino acid-defined diet identified glycine as the only amino acid that decreased with age (Figure S6B) and the levels were not influenced by sex (Figure S6C). Interestingly, the decrease in serine abundance in human skeletal muscle biopsy tissue was not paralleled by a decrease in the expression of serine synthesis enzyme genes (Figure S6D). Thus, we considered that both circulating and skeletal muscle amino acid availability could affect MuSC/MPCs when the myofiber membrane is disrupted with injury [56,57]. Next we sought to determine whether dietary serine and glycine intake could further diminish circulating and skeletal muscle serine/glycine availability and augment age-related impairments in skeletal muscle regeneration. Aged mice (>20 mo) under dietary serine/glycine restriction recapitulated the human serine/glycine phenotype (Figure 6BCD). Compared to the young mice, the aged mice had reduced MuSC abundance at 3 dpi (Figure S6E), similar to previous observations. During the Ser/Gly_{depleted} diet, the aged mice had a trend of even fewer MuSCs at 3 dpi ($p = 0.06$, Figure 6EF) following a similar pattern as observed in the young mice. At 28 dpi, when skeletal muscle regeneration should be nearing completion, the aged mice fed the Ser/Gly_{depleted} diet had no detectable differences in myofiber size (Figure 6GH). Strikingly, the aged mice fed the Ser/Gly_{depleted} diet had pronounced intermyocellular adipocyte infiltration, which we confirmed with PERILIPIN-1 staining (Figure 6GI). The increase in adipocyte infiltration was specific to the injured muscle; there was no significant change in the whole body composition (Figure S6F). These results support monitoring levels of dietary serine/glycine as a standard of care post-muscle injury/surgery for older adults.

4. DISCUSSION

In this study, we report that extracellular serine/glycine are indispensable for *h*MPC proliferation, MuSC abundance, and skeletal muscle regeneration post-injury. The serine/glycine auxotrophy demonstrated by *h*MPCs was in alignment with previous reports using murine myoblast cell lines [58,59]. Our research extends these previous findings by demonstrating that *de novo* serine/glycine biosynthesis occurs in MPCs but only at levels sufficient for survival when extracellular concentrations are limited. Furthermore, we demonstrated that dietary restriction of serine/glycine reduced skeletal muscle and circulating levels of serine and MuSC abundance 3 dpi in the young and old healthy mice. In a model of disrupted serine/glycine availability, we demonstrated that skeletal muscle pathological remodeling with enhanced adipocyte infiltration results post-injury with diminished serine/glycine concentration. Our results in MuSCs/MPCs support studies in non-muscle cells that demonstrate a requirement for serine/glycine for cell proliferation and function during physiological challenge.

For the first time, we identified that *h*MPCs possess the capacity for *de novo* serine/glycine biosynthesis. Intriguingly, we note that serine/glycine biosynthesis occurs when *h*MPCs are challenged with extracellular serine/glycine restriction. Furthermore, when serine/glycine biosynthesis occurs, it is ineffective at restoring intracellular levels of serine/glycine to a degree necessary to support proliferation. Intriguingly, serine/glycine restriction did not increase glucose uptake nor did increasing levels of available glucose influence *h*MPC proliferation, suggesting a disconnect between available substrate and biosynthesis capacity. We note that serine/glycine restriction did not increase cell death and therefore the limited ability of serine/glycine biosynthesis by MuSC/MPCs in serine/glycine restricted conditions is adequate to support cell survival. Therefore, it is likely that the decline in serine/glycine availability in the MuSC/MPC extracellular environment observed with aging and chronic disease conditions, coupled with the

limited capacity for MuSC/MPC *de novo* serine/glycine biosynthesis, may be a causal factor in the limited skeletal muscle regeneration efficiency observed in older individuals [2] as well as those with CKD [3], type I diabetes [4,5], and muscle dystrophy [6].

This study supports a growing body of literature demonstrating that dietary glycine supplementation protects muscle mass and function in a number of disease and aberrant metabolic states [22–26]. To date, the beneficial effects of glycine supplementation on skeletal muscle in the disease state has been attributed to glycine's systemic anti-inflammatory effects, its contribution to balancing ROS signaling in whole skeletal muscle tissue, and its ability to restore skeletal muscle's anabolic response to leucine [60]. Our research suggests this benefit may also be conferred by a direct benefit to MuSC/MPC proliferative capacity, which supports a recent report that identified the beneficial effects of glycine supplementation on muscle regeneration in a model of muscle dystrophy is conferred in part by enhancements in MPC proliferation [24].

The ability of MuSC/MPCs to buffer ROS produced as a natural consequence of proliferation [61] relies in part on extracellular serine/glycine used for glutathione synthesis. The necessity of glutathione synthesis for MuSC/MPC population expansion was supported by experiments that demonstrated a reduction in *h*MPC population expansion when glutathione synthesis was inhibited, even in the presence of serine/glycine (Figure 4HI). Additionally, the reliance on glutathione synthesis to maintain proliferation was triangulated by our experiments in which supplementation of cell-permeable glutathione increased *h*MPC numbers in a modest but repeatable manner in the absence of extracellular serine/glycine. Furthermore, ROS production may have been upregulated beyond normal levels in a compensatory manner in response to cell cycle arrest in the absence of serine/glycine [62], further reducing glutathione levels. There is evidence that dietary interventions help maintain glutathione levels with advancing age. For example, a persistent metabolic phenotype associated with aging is increased ROS due to impaired glutathione synthesis, which is correctable in red blood cells with dietary supplementation of the glutathione precursors glycine and cysteine [63]. Future studies should examine the efficacy of dietary serine/glycine supplementation to improve glutathione production and subsequently MuSC/MPC proliferation during skeletal muscle regeneration in individuals with reduced endogenous serine and glycine.

We demonstrated that limited intracellular serine/glycine and/or subsequent alterations in intracellular metabolism is sensed in a p-eIF2 α -dependent manner, resulting in halted protein synthesis and cell cycle arrest. eIF2 α , a translation initiation factor responsive to cell extrinsic and intrinsic stress signals, selectively enhances the translation of ATF4, which in turn upregulates the transcription of genes associated with metabolism and nutrient uptake [64]. Stress signals observed in this study, including inadequate amino acid availability and elevated ROS, activate the integrated stress response. While not specifically evaluated herein, we hypothesize that limited serine/glycine availability enhanced general control non-repressible 2 (GCN2) activity and subsequently the phosphorylation of eIF2 α through sensing an accumulation of uncharged tRNAs [65] or stalled ribosomes [66]. Additionally, it has been proposed that the upstream target of eIF2 α , protein kinase R-like endoplasmic reticulum kinase (PERK), is responsive to intracellular ROS levels, leading to eIF2 α phosphorylation and translation of ATF4 [64,67]. Therefore, it remains unknown whether the stress signal that elicited the eIF2 α /ATF4 response in *h*MPCs in the present study was the low levels of serine/glycine themselves, the buildup of intracellular ROS, or through another mechanism.

The uniform proliferative response of *h*MPCs from various donors in response to extracellular serine/glycine coupled with the relative safety of short-term serine/glycine [68] indicate that future clinical applications of these amino acids as therapeutics to improve muscle regeneration are viable. Currently, dietary serine and glycine standardization or supplementation are not a part of standard care post-skeletal muscle trauma/surgery despite the observation that the availability of endogenous serine and potentially glycine is strongly influenced by the diet [44,45]. Standardization or supplementation of dietary serine/glycine is important to consider given that aged adults and adults with various pathologies are unable to maintain endogenous serine and glycine levels [12–14,16,17]. While the source of age- and disease-related decreases in serine/glycine availability in circulation/skeletal muscle tissue remains an open question, it may be due to increased metabolic demand [69]. Another potential source of decreased serine/glycine levels that we observed in skeletal muscle may be dysregulation of expression of serine/glycine biosynthesis enzymes or nutrient transporters [70], although we noted no decrease in the expression of serine biosynthesis enzymes in skeletal muscle tissue with age (Fig. S6D). Alternatively, while gastrointestinal absorption of amino acids after feeding is not impaired with age [71,72], overall protein intake does decrease [73], suggesting that reduced intake may drive reduced serine/glycine availability. Attractive targets for future clinical studies include evaluation of the efficacy of short-term serine/glycine supplementation during times of robust skeletal muscle regeneration including after surgical procedures [74] and burn injuries [75]; however, more *in vivo* studies are needed to determine the timing and dosage of serine/glycine to overcome a deficient diet. While positive preclinical data already exist evaluating the long-term effect of glycine supplementation for lifespan extension [69], the recent loss of the generally regarded as safe (GRAS) status for glycine (CFR Title 21 Section 170.50) makes long-term supplementation unattractive, indicating that treatment within the short-term window for tissue regeneration would be ideal.

5. CONCLUSION

In conclusion, we have outlined a novel requirement for extracellular serine/glycine to support MPC/MuSC proliferation. Furthermore, we have identified that dietary standardization of increased levels of serine and glycine may be necessary as part of standard care post-skeletal muscle trauma for populations (e.g., aged adults) who are unable to maintain their endogenous serine and glycine levels.

DATA AVAILABILITY

All the transcriptomic data generated or analyzed in the present study are included in this article (and the accompanying supplementary files). Additional data supporting the findings described in this article are available from the corresponding author upon reasonable request and the raw RNA sequencing data have been deposited in the NCBI Gene Expression Omnibus database (GSE161357).

AUTHOR CONTRIBUTIONS

Conceptualization: B.J.G, P.J.S, and A.E.T. Methodology: B.J.G, B.D.C, M.S.F., P.J.S, M.S.A., and A.E.T. Investigation: B.J.G, J.E.B, M.E.G., E.W.L., M.K.H., E.H.H.F, A.K., S.K, M.E.G., and E.L.B. Resources: E.B., P.J.S, M.S.F., B.D.C., C.M.M., and A.E.T. Writing original draft: B.J.G. and A.E.T. Writing, review, and editing: B.J.G., J.E.B, M.E.G., E.W.L., M.K.H., P.J.S., M.S.F., B.D.C., C.M.M., and A.E.T. Supervision: A.E.T.

ACKNOWLEDGMENTS

This study was financially supported by a President's Council of Cornell Women Award (to A.T.M), Cornell University Division of Nutritional Sciences funds (to A.T.M), a Canadian Institutes for Health Research Doctoral Foreign Study Award (to B.J.G), the National Science Foundation Graduate Research Fellowship Program under grant no. DGE-1650441 (to J.E.B.), a Glenn Medical Research Foundation and American Federation for Aging Research Grant for Junior Faculty (to B.D.C.), and the National Institutes of Health under awards R01AG058630 (to B.D.C. and A.T.M.), R21AR072265 (to B.D.C.), and R01CA234245 (to C.M.M.).

CONFLICT OF INTEREST

The authors declare no conflicts of interest.

APPENDIX A. SUPPLEMENTARY DATA

Supplementary data to this article can be found online at <https://doi.org/10.1016/j.molmet.2020.101106>.

REFERENCES

- [1] Seale, P., Sabourin, L.A., Girgis-Gabardo, A., Mansouri, A., Gruss, P., Rudnicki, M.A., 2000. Pax7 is required for the specification of myogenic satellite cells. *Cell* 102(6):777–786.
- [2] Sadeh, M., 1988. Effects of aging on skeletal muscle regeneration. *Journal of Neurological Sciences* 87(1):67–74.
- [3] Zhang, L., Wang, X.H., Wang, H., Du, J., Mitch, W.E., 2010. Satellite cell dysfunction and impaired IGF-1 signaling cause CKD-induced muscle atrophy. *Journal of the American Society of Nephrology* 21(3):419–427.
- [4] Krause, M.P., Al-Sajee, D., D'Souza, D.M., Rebalka, I.A., Moradi, J., Riddell, M.C., et al., 2013. Impaired macrophage and satellite cell infiltration occurs in a muscle-specific fashion following injury in diabetic skeletal muscle. *PLoS One* 8(8):e70971.
- [5] Krause, M.P., Moradi, J., Nissar, A.A., Riddell, M.C., Hawke, T.J., 2011. Inhibition of plasminogen activator inhibitor-1 restores skeletal muscle regeneration in untreated type 1 diabetic mice. *Diabetes* 60(7):1964–1972.
- [6] Carnwath, J.W., Shotton, D.M., 1987. Muscular dystrophy in the mdx mouse: histopathology of the soleus and extensor digitorum longus muscles. *Journal of Neurological Sciences* 80(1):39–54.
- [7] Blau, H.M., Cosgrove, B.D., Ho, A.T.V., 2015. The central role of muscle stem cells in regenerative failure with aging. *Nature Medicine* 21(8):854–862.
- [8] Dumont, N.A., Wang, Y.X., Rudnicki, M.A., 2015. Intrinsic and extrinsic mechanisms regulating satellite cell function. *Development* 142(9):1572–1581.
- [9] Chakkalakal, J.V., Jones, K.M., Basson, M.A., Brack, A.S., 2012. The aged niche disrupts muscle stem cell quiescence. *Nature* 490(7420):355–360.
- [10] Conboy, I.H., Conboy, M.J., Smythe, G.M., Rando, T.A., 2003. Notch-Mediated restoration of regenerative potential to aged muscle. *Science* 302(5650):1575–1577.
- [11] Elabd, C., Cousin, W., Upadhyayula, P., Chen, R.Y., Chooljian, M.S., Li, J., et al., 2014. Oxytocin is an age-specific circulating hormone that is necessary for muscle maintenance and regeneration. *Nature Communications* 5:4082.
- [12] Spitali, P., Hettne, K., Tsonaka, R., Sabir, E., Seyer, A., Hemerik, J.B.A., et al., 2018. Cross-sectional serum metabolomic study of multiple forms of muscular dystrophy. *Journal of Cellular and Molecular Medicine* 22(4):2442–2448.
- [13] Houtkooper, R.H., Argmann, C., Houten, S.M., Canto, C., Jenjina, E.H., Andreux P erielope, A., et al., 2011. The metabolic footprint of aging in mice. *Scientific Reports* 1:134.

- [14] Yan-Do, R., MacDonald, P.E., 2017. Impaired “glycine”-mia in type 2 diabetes and potential mechanisms contributing to glucose homeostasis. *Endocrinology* 158(5):1064–1073.
- [15] Hosios, A.M., Hecht, V.C., Danai, L.V., Johnson, M.O., Rathmell, J.C., Steinhauser, M.L., et al., 2016. Amino acids rather than glucose account for the majority of cell mass in proliferating mammalian cells. *Developmental Cell* 36(5):540–549.
- [16] Kouchiwa, T., Wada, K., Uchiyama, M., Kasezawa, N., Niisato, M., Murakami, H., et al., 2012. Age-related changes in serum amino acids concentrations in healthy individuals. *Clinical Chemistry and Laboratory Medicine* 50(5):861–870.
- [17] Zeng, L., Yu, Y., Cai, X., Xie, S., Chen, J., Zhong, L., et al., 2019. Differences in serum amino acid phenotypes among patients with diabetic nephropathy, hypertensive nephropathy, and chronic nephritis. *Medical Science Monitor* 25: 7235–7242.
- [18] Labuschagne, C.F., van den Broek, N.J.F., Mackay, G.M., Vousden, K.H., Maddocks, O.D.K., 2014. Serine, but not glycine, supports one-carbon metabolism and proliferation of cancer cells. *Cell Reports* 7(4):1248–1258.
- [19] Maddocks, O.D.K., Berkers, C.R., Mason, S.M., Zheng, L., Blyth, K., Gottlieb, E., et al., 2013. Serine starvation induces stress and p53-dependent metabolic remodelling in cancer cells. *Nature* 493(7433):542–546.
- [20] Diehl, F.F., Lewis, C.A., Fiske, B.P., Vander Heiden, M.G., 2019. Cellular redox state constrains serine synthesis and nucleotide production to impact cell proliferation. *Nature Metabolism* 1(9):861–867.
- [21] Ma, E.H., Bantug, G., Griss, T., Condotta, S., Johnson, R.M., Samborska, B., et al., 2017. Serine is an essential metabolite for effector T cell expansion. *Cell Metabolism* 25(2):345–357.
- [22] Ham, D.J., Murphy, K.T., Chee, A., Lynch, G.S., Koopman, R., 2014. Glycine administration attenuates skeletal muscle wasting in a mouse model of cancer cachexia. *Clinical Nutrition* 33(3):448–458.
- [23] Ham, D.J., Gardner, A., Kennedy, T.L., Trieu, J., Naim, T., Chee, A., et al., 2019. Glycine administration attenuates progression of dystrophic pathology in prednisolone-treated dystrophin/utrophin null mice. *Scientific Reports* 9(1): 12982.
- [24] Lin, C., Han, G., Ning, H., Song, J., Ran, N., Yi, X., et al., 2020. Glycine enhances satellite cell proliferation, cell transplantation and oligonucleotide efficacy in dystrophic muscle. *Molecular Therapy* 6(5):1339–1358.
- [25] Ham, D.J., Caldwell, M.K., Chhen, V., Chee, A., Wang, X., Proud, C.G., et al., 2016. Glycine restores the anabolic response to leucine in a mouse model of acute inflammation. *American Journal of Physiology. Endocrinology and Metabolism* 310(11):E970–E981.
- [26] Caldwell, M.K., Ham, D.J., Godeassi, D.P., Chee, A., Lynch, G.S., Koopman, R., 2016. Glycine supplementation during calorie restriction accelerates fat loss and protects against further muscle loss in obese mice. *Clinical Nutrition* 35(5): 1118–1126.
- [27] Riddle, E.S., Bender, E.L., Thalacker-Mercer, A.E., 2018. Expansion capacity of human muscle progenitor cells differs by age, sex, and metabolic fuel preference. *American Journal of Physiology—Cell Physiology* 315(5):C643–C652.
- [28] Gheller, B.J., Blum, J.E., Merritt, E.K., Cummings, B.P., Thalacker-Mercer, A.E., Peptide, Y.Y., 2019. (PYY) is expressed in human skeletal muscle tissue and expanding human muscle progenitor cells. *Frontiers in Physiology* 10:188.
- [29] Riddle, E.S., Bender, E.L., Thalacker-Mercer, A.E., 2018. Transcript profile distinguishes variability in human myogenic progenitor cell expansion capacity. *Physiological Genomics* 50(10):817–827.
- [30] Gheller, B.J., Blum, J., Soueid-Baumgarten, S., Bender, E., Cosgrove, B.D., Thalacker-Mercer, A., 2019. Isolation, culture, characterization, and differentiation of human muscle progenitor cells from the skeletal muscle biopsy procedure. *Journal of Visualized Experiments* (150).
- [31] Xu, X., Wilschut, K.J., Kouklis, G., Tian, H., Hesse, R., Garland, C., et al., 2015. Human satellite cell transplantation and regeneration from diverse skeletal muscles. *Stem Cell Reports* 5(3):419–434.
- [32] Wallace, M., Green, C., Roberts, L., Lee, Y., McCarville, J., Sanchez-Gurmaches, J., et al., 2018. Enzyme promiscuity drives branched-chain fatty acid synthesis in adipose tissues. *Nature Chemical Biology* 14(11):1021–1031.
- [33] Schindelin, J., Arganda-Carreras, I., Frise, E., Kaynig, V., Longair, M., Pietzsch, T., et al., 2012. Fiji: an open-source platform for biological-image analysis. *Nature Methods* 9:676–682.
- [34] Briguet, A., Courdier-Fruh, I., Foster, M., Meier, T., Magyar, J.P., 2004. Histological parameters for the quantitative assessment of muscular dystrophy in the mdx-mouse. *Neuromuscular Disorders* 14(10):675–682.
- [35] Kawakami, A., Kimura-Kawakami, M., Nomura, T., Fujisawa, H., 1997. Distributions of PAX6 and PAX7 proteins suggest their involvement in both early and late phases of chick brain development. *Mechanisms of Development* 66(1–2):119–130.
- [36] Martin, M., 2011. Cutadapt removes adapter sequences from high-throughput sequencing reads. *EMBnetjournal* 17(1):10.
- [37] Kim, D., Pertea, G., Trapnell, C., Pimentel, H., Kelley, R., Salzberg, S.L., 2013. TopHat2: accurate alignment of transcriptomes in the presence of insertions, deletions and gene fusions. *Genome Biology* 4(4):14.
- [38] McCarthy, D.J., Chen, Y., Smyth, G.K., 2012. Differential expression analysis of multifactor RNA-Seq experiments with respect to biological variation. *Nucleic Acids Research* 40(10):4288–4297.
- [39] Woeller, C.F., Anderson, D.D., Szebenyi, D.M.E., Stover, P.J., 2007. Evidence for small ubiquitin-like modifier-dependent nuclear import of the thymidylate biosynthesis pathway. *Journal of Biological Chemistry* 282(24):17623–17631.
- [40] Anderson, D.D., Stover, P.J., 2009. SHMT1 and SHMT2 are functionally redundant in nuclear de novo thymidylate biosynthesis. *PLoS One* 6(6):4.
- [41] Wright, W.E., Binder, M., Funk, W., 1991. Cyclic amplification and selection of targets (CASTing) for the myogenin consensus binding site. *Molecular and Cellular Biology* 11(8):4104–4110.
- [42] Cordes, T., Metallo, C.M., 2019. Quantifying intermediary metabolism and lipogenesis in cultured mammalian cells using stable isotope tracing and mass spectrometry. In: *Methods in Molecular Biology*. p. 219–41.
- [43] Schmidt, E.K., Clavarino, G., Ceppi, M., Pierre, P., 2009. SUnSET, a nonradioactive method to monitor protein synthesis. *Nature Methods* 6(4): 275–277.
- [44] Henrich, C.J., 2016. A microplate-based nonradioactive protein synthesis assay: application to TRAIL sensitization by protein synthesis inhibitors. *PLoS One* 10(10):11.
- [45] Gannon, M.C., Nuttall, J.A., Nuttall, F.Q., 2002. The metabolic response to ingested glycine. *American Journal of Clinical Nutrition* 76(6):1302–1307.
- [46] Garofalo, K., Penno, A., Schmidt, B.P., Lee, H.J., Frosch, M.P., Von Eckardstein, A., et al., 2011. Oral L-serine supplementation reduces production of neurotoxic deoxysphingolipids in mice and humans with hereditary sensory autonomic neuropathy type 1. *Journal of Clinical Investigation* 121(12):4735–4745.
- [47] Bergstrom, J., Furst, P., Noree, L.O., Vinnars, E., 1974. Intracellular free amino acid concentration in human muscle tissue. *Journal of Applied Physiology* 36(6):693–697.
- [48] Pavlidou, T., Rosina, M., Fuoco, C., Gerini, G., Gargioli, C., Castagnoli, L., et al., 2017. Regulation of myoblast differentiation by metabolic perturbations induced by metformin. *PLoS One* 8(8):12.
- [49] Kitzmann, M., Carnac, G., Vandromme, M., Primig, M., Lamb, N.J.C., Fernandez, A., 1998. The muscle regulatory factors MyoD and Myf-5 undergo distinct cell cycle-specific expression in muscle cells. *The Journal of Cell Biology* 142(6):1447–1459.
- [50] Herbig, K., Chiang, E.P., Lee, L.R., Hills, J., Shane, B., Stover, P.J., 2002. Cytoplasmic serine hydroxymethyltransferase mediates competition between folate-dependent deoxyribonucleotide and S-adenosylmethionine biosyntheses. *Journal of Biological Chemistry* 277(41):38381–38389.

- [51] Field, M.S., Kamynina, E., Agunloye, O.C., Liebenthal, R.P., Lammare, S.G., Brosnan, M.E., et al., 2014. Nuclear enrichment of folate cofactors and methylenetetrahydrofolate dehydrogenase 1 (MTHFD1) protect de novo thymidylate biosynthesis during folate deficiency. *Journal of Biological Chemistry* 289(43):29642–29650.
- [52] DeNicola, G.M., Chen, P.H., Mullarky, E., Sudderth, J.A., Hu, Z., Wu, D., et al., 2015. NRF2 regulates serine biosynthesis in non-small cell lung cancer. *Nature Genetics* 47(12):1475–1481.
- [53] Holcik, M., Sonenberg, N., 2005. Translational control in stress and apoptosis. *Nature Reviews Molecular Cell Biology* 6(4):318–327.
- [54] Polymenis, M., Aramayo, R., 2015. Translate to divide: control of the cell cycle by protein synthesis. *Microbial Cell* 2:94–104.
- [55] Sidrauski, C., McGeachy, A.M., Ingolia, N.T., Walter, P., 2015. The small molecule ISRIB reverses the effects of eIF2 α phosphorylation on translation and stress granule assembly. *Elife* (4):e05033.
- [56] Dixon, R.W., Harris, J.B., 1996. Myotoxic activity of the toxic phospholipase, notexin, from the venom of the Australian tiger snake. *Journal of Neuro-pathology & Experimental Neurology* 55(12):1230–1237.
- [57] Morton, A.B., Norton, C.E., Jacobsen, N.L., Fernando, C.A., Cornelison, D.D.W., Segal, S.S., 2019. Barium chloride injures myofibers through calcium-induced proteolysis with fragmentation of motor nerves and microvessels. *Skeletal Muscle* 9(1):27.
- [58] Dufresne, M.J.P., MacLeod, J., Rogers, J., Sanwal, B.D., 1976. Serine auxotrophy of myoblasts in primary and secondary culture. *Biochemical and Biophysical Research Communications* 70(4):1085–1090.
- [59] Sun, K., Wu, Z., Ji, Y., Wu, G., 2016. Glycine regulates protein turnover by activating protein kinase B/mammalian target of rapamycin and by inhibiting MuRF1 and atrogin-1 gene expression in C2C12 myoblasts. *Journal of Nutrition* 146(12):2461–2467.
- [60] Koopman, R., Caldwell, M.K., Ham, D.J., Lynch, G.S., 2017. Current opinion in clinical nutrition and metabolic care. Glycine metabolism in skeletal muscle: Implications for metabolic homeostasis 20:237–242.
- [61] L'Honoré, A., Commère, P.H., Negroni, E., Pallafacchina, G., Friguet, B., Drouin, J., et al., 2018. The role of Pitx2 and Pitx3 in muscle 1 stem cells gives new insights into P38 α MAP kinase and redox regulation of muscle regeneration. *Elife* 7:e32991.
- [62] Sciancalepore, M., Luin, E., Parato, G., Ren, E., Giniatullin, R., Fabbretti, E., et al., 2012. Reactive oxygen species contribute to the promotion of the ATP-mediated proliferation of mouse skeletal myoblasts. *Free Radical Biology and Medicine* 53(7):1392–1398.
- [63] Sekhar, R.V., Patel, S.G., Guthikonda, A.P., Reid, M., Balasubramanyam, A., Taffet, G.E., et al., 2011. Deficient synthesis of glutathione underlies oxidative stress in aging and can be corrected by dietary cysteine and glycine supplementation. *American Journal of Clinical Nutrition* 94(3):847–853.
- [64] Harding, H.P., Zhang, Y., Zeng, H., Novoa, I., Lu, P.D., Calfon, M., et al., 2003. An integrated stress response regulates amino acid metabolism and resistance to oxidative stress. *Molecular Cell* 11(3):619–633.
- [65] Wek, S.A., Zhu, S., Wek, R.C., 1995. The histidyl-tRNA synthetase-related sequence in the eIF-2 alpha protein kinase GCN2 interacts with tRNA and is required for activation in response to starvation for different amino acids. *Molecular and Cellular Biology* 15(8):4497–4506.
- [66] Inglis, A.J., Masson, G.R., Shao, S., Perisic, O., McLaughlin, S.H., Hegde, R.S., et al., 2019. Activation of GCN2 by the ribosomal P-stalk. *Proceedings of the National Academy of Sciences of the U S A* 116(11):4946–4954.
- [67] Avivar-Valderas, A., Salas, E., Bobrovnikova-Marjon, E., Diehl, J.A., Nagi, C., Debnath, J., et al., 2011. PERK integrates autophagy and oxidative stress responses to promote survival during extracellular matrix detachment. *Molecular and Cellular Biology* 31(17):3616–3629.
- [68] Levine, T.D., Miller, R.G., Bradley, W.G., Moore, D.H., Saperstein, D.S., Flynn, L.E., et al., 2017. Phase I clinical trial of safety of L-serine for ALS patients. *Amyotroph Lateral Scler Front Degener* 18(1–2):107–111.
- [69] Miller, R.A., Harrison, D.E., Astle, C.M., Bogue, M.A., Brind, J., Fernandez, E., et al., 2019. Glycine supplementation extends lifespan of male and female mice. *Aging Cell* 18(3):e12953.
- [70] Kawase, A., Ito, A., Yamada, A., Iwaki, M., 2015. Age-related changes in mRNA levels of hepatic transporters, cytochrome P450 and UDP-glucuronosyltransferase in female rats. *European Journal of Drug Metabolism and Pharmacokinetics* 40(2):239–244.
- [71] Mitchell, W.K., Phillips, B.E., Williams, J.P., Rankin, D., Lund, J.N., Wilkinson, D.J., et al., 2015. The impact of delivery profile of essential amino acids upon skeletal muscle protein synthesis in older men: clinical efficacy of pulse vs. bolus supply. *American Journal of Physiology. Endocrinology and Metabolism* 309(5):E450–E457.
- [72] Katsanos, C.S., Kobayashi, H., Sheffield-Moore, M., Aarsland, A., Wolfe, R.R., 2006. A high proportion of leucine is required for optimal stimulation of the rate of muscle protein synthesis by essential amino acids in the elderly. *American Journal of Physiology. Endocrinology and Metabolism* 291(2):E381–E387.
- [73] Krok-Schoen, J.L., Archdeacon Price, A., Luo, M., Kelly, O.J., Taylor, C.A., 2019. Low dietary protein intakes and associated dietary patterns and functional limitations in an aging population: a NHANES analysis. *The Journal of Nutrition, Health & Aging* 23(4):338–347.
- [74] Qazi, T.H., Duda, G.N., Ort, M.J., Perka, C., Geissler, S., Winkler, T., 2019. Cell therapy to improve regeneration of skeletal muscle injuries. *Journal of Cachexia, Sarcopenia and Muscle* 10:501–516.
- [75] Fry, C.S., Porter, C., Sidossis, L.S., Nieten, C., Reidy, P.T., Hundeshagen, G., et al., 2016. Satellite cell activation and apoptosis in skeletal muscle from severely burned children. *The Journal of Physiology* 594(18):5223–5236.